RESEARCH ARTICLE

Landscape patterns from mathematical morphology on maps with contagion

Kurt Riitters · Peter Vogt · Pierre Soille · Christine Estreguil

Abstract The perceived realism of simulated maps with contagion (spatial autocorrelation) has led to their use for comparing landscape pattern metrics and as habitat maps for modeling organism movement across landscapes. The objective of this study was to conduct a neutral model analysis of pattern metrics defined by morphological spatial pattern analysis (MSPA) on maps with contagion, with comparisons to phase transitions (abrupt changes) of patterns on simple random maps. Using MSPA, each focal class pixel on a neutral map was assigned to one of six pattern classes—core, edge, perforated, connector, branch, or islet—depending on MSPA rules for connectivity and edge width. As the density of the focal class (P) was increased on simple random maps, the proportions of pixels in different pattern classes exhibited two types of phase transitions at threshold densities ($0.41 \leq P \leq 0.99$) that were predicted by percolation theory after taking into account the MSPA rules for connectivity and edge width. While there was no evidence of phase transitions on maps with contagion, the general trends of pattern metrics in relation to P were similar to simple random maps. Using an index P for comparisons, the effect of increasing contagion was opposite that of increasing edge width.

Keywords Pattern analysis · Neutral model · Percolation theory · Phase transition · Simulation · Threshold

K. Riitters (✉)
US Department of Agriculture, Forest Service, Southern Research Station, 3041 Cornwallis Road, Research Triangle Park, NC 27709, USA
e-mail: kriitters@fs.fed.us

P. Vogt · C. Estreguil
European Commission, Joint Research Centre, Institute for Environment and Sustainability, T.P. 261, Via E. Fermi 2749, 21027 Ispra (VA), Italy

P. Soille
European Commission, Joint Research Centre, Institute for the Protection and Security of the Citizen, T.P. 267, Via E. Fermi 2749, 21027 Ispra (VA), Italy

Introduction

It is necessary to test new pattern metrics and applications of them on neutral maps because testing a pattern-process hypothesis requires knowledge of the expected pattern without the process (Gardner et al. 1987; With and King 1997; Gardner and Urban 2007). The pattern metrics developed by Vogt et al. (2007a, b) from mathematical morphology (Serra 1982; Soille 2003) have been tested with simple random neutral maps (Riitters et al. 2007). The objective of this study was to extend those tests to more realistic neutral maps that exhibit contagion (spatial autocorrelation), while incorporating improvements to the pattern metrics (Soille and Vogt 2009). Of particular interest were

comparisons of the phase transitions (abrupt changes) of pattern metrics which occur on simple random maps (Riitters et al. 2007). That is of interest because phase transitions of landscape patterns may be linked to phase transitions of ecological functions that depend on patterns (O'Neill et al. 1988; Gardner et al. 1989). Knowledge of the associated thresholds for landscape patterns on neutral maps with contagion may help to predict critical thresholds in many ecological phenomena in real landscapes (With and King 1997) which is a central problem in ecology (Burkett et al. 2005; Groffman et al. 2006).

Keitt (2000) defined a neutral map as a stochastic model of a spatial pattern where the value assigned to any location in the pattern is a random variable, regardless of any constraints placed on that variable. The most common neutral map in landscape ecology is a simple random map, but neutral maps with contagion are also popular because contagion is a fundamental aspect of landscape pattern. Neutral maps exhibiting a range of contagion have been used, for example, as test-beds for comparing landscape pattern metrics (Gustafson and Parker 1992; Neel et al. 2004; Ferrari et al. 2007), and as habitat maps for models of organism movement (With and King 2001; King and With 2002). We included both simple random maps and 'multifractal' maps produced by the RULE software (Gardner 1999) in this study. The maps are 'neutral' in the sense that they are random ensembles of maps whose properties are described by statistical averages (Keitt 2000), and the 'multifractal' maps are 'with contagion' in the sense that different values of the RULE parameters P (proportion of the map that is the focal class) and H (Hurst exponent) produce maps with varying degrees of focal class clumping (Gardner 1999).

We applied percolation theory (e.g., Stauffer 1985) as a framework for interpreting the analyses of neutral maps. Percolation theory considers the probability of a connection between any two locations, which depends on the density of locations (P), the relative positions of the two locations (e.g., independent vs. spatially correlated placement), the lattice geometry (e.g., hexagonal vs. square locations), and the connectivity rule (e.g., 4- vs. 8-neighbor). Overall connectedness is indicated by the existence of a percolating state, defined as the existence of a map-spanning connected cluster of focal class locations. The transition between a non-percolating state and a

percolating state is a phase transition, and it occurs at a threshold P that is determined by the other system parameters (e.g., Plotnick and Gardner 1993). With (2002) provided an ecological review of the concepts and applications of percolation theory which, like the early applications by O'Neill et al. (1988), Gardner et al. (1989), and O'Neill et al. (1992), have mainly addressed landscape connectedness as it affects resource utilization and population dispersal. Applications of percolation theory are relatively easy in the case of simple random maps, but maps with contagion present the more difficult problem of 'correlated percolation' (e.g., Essam 1980) which remains an active research topic (e.g., Frary and Schuh 2007).

We examined the pattern metrics which come from the application of morphological spatial pattern analysis (MSPA) to raster maps (Soille and Vogt 2009). Briefly, the set of focal class (e.g., 'habitat') pixels is separated into mutually exclusive subsets according to the structural roles that the subsets play on a map. For example, the subset of 'connector' pixels forms structural paths between the subset of 'core' pixels. We refer to those subsets as 'pattern classes' and we consider the six MSPA pattern classes called 'core,' 'edge,' 'perforation,' 'connector,' 'branch,' and 'islet' (Soille and Vogt 2009). MSPA has two parameters to define focal class connectivity and analysis scale.

Earlier analyses of MSPA pattern classes on simple random neutral maps (Riitters et al. 2007) considered 4-neighbor focal class connectivity and varied the analysis scale by changing the size of the 'structuring element' (Vogt et al. 2007a). There were two phase transitions involving MSPA pattern classes that were explained by percolation theory in light of the definitions of the pattern classes and the MSPA parameters. The first type of phase transition signaled a change in overall connectedness by shifts of pixels between the 'patch' and the 'connector' plus 'branch' pattern classes, and corresponded to the classical phase transition of the percolating state of all focal class pixels. The second type of phase transition signaled a change in edge context from interior to exterior, by shifts of pixels between the 'edge' and the 'perforated' pattern classes, and corresponded to a phase transition of the percolating state of the complement of the 'core' pattern class pixels including the pixels that were not in the focal class. In this

study, we considered 8-neighbor focal class connectivity and varied the analysis scale by changing the 'edge width' (Ostapowicz et al. 2008; Soille and Vogt 2009). Since those differences were likely to affect the phase transitions and threshold values that were observed before, we included both simple random maps and maps with contagion for comparisons.

Comparisons of different types of neutral maps in a percolation theory framework require methods to detect phase transitions and to estimate the associated threshold densities. On infinite maps, phase transitions are defined mathematically by the probability that a given location is connected to an infinite cluster. As the density is increased while holding other system parameters constant, a threshold density is reached at which that probability changes from zero to non-zero, which can only occur at the phase transition corresponding to the emergence of an infinite cluster. As a practical matter, phase transitions on finite maps are usually detected by direct observation of the emergence of a map-spanning cluster, or by indirect observation of an abrupt change in an 'order parameter' which is simply a pattern metric (e.g., the size of the largest cluster, or the correlation length) that is sensitive to the existence of a map-spanning cluster.

The problem in the analysis of neutral maps is to identify phase transitions and thresholds based on the statistical properties of random samples of finite maps that differ only in the focal class density (P). In the case of simple random maps, a phase transition always occurs near the same threshold density for all maps because all finite simple random maps are a sample from the same infinite map. That means that an abrupt change in either the proportion of maps that exhibit a map-spanning cluster, the mean value of an order parameter, or the between-map variance of an order parameter are all robust indicators of phase transitions and thresholds on simple random maps. The estimation problem is more difficult in the case of RULE-generated maps with contagion because all finite sample maps do not come from the same infinite map. As a result, the map-spanning cluster does not usually emerge near the same threshold density on all maps in a sample.

In that case, a common convention is to estimate a threshold density as the value of P at which 50% of the maps exhibit a map-spanning cluster (e.g., With 2002, 2004). While that estimator is robust on simple

random maps, it is biased on maps with contagion (e.g., Chaves and Koiller 1995; Frary and Schuh 2007). Another problem is that threshold estimates can vary substantially if the convention is that 100% (instead of 50%) of the maps exhibit a map-spanning cluster (Ferrari et al. 2007). While such estimates can be used as 'index values' to compare maps exhibiting a range of contagion (e.g., With 2002), they can not be compared directly to thresholds for simple random maps. Considering the use of order parameters to detect phase transitions and estimate thresholds, abrupt changes in the means or variances of pattern metrics are not typical for samples of neutral maps with contagion. For example, Neel et al. (2004) reported "threshold-like behavior" and "nonlinear behavior associated with the percolation threshold" for several pattern metrics, but concluded that abrupt changes indicating phase transitions were "dampened" by contagion.

Since our objective was to compare maps with contagion to simple random maps, we were compelled to use the same methods for both. Furthermore, since we also wanted to compare results to earlier analyses of simple random maps, it was necessary to use the same methods as before. The proportions of focal class pixels in the six MSPA pattern classes were considered to be order parameters, and inferences about phase transitions and thresholds were based on abrupt shifts in those proportions in relation to P, accompanied by 'variance spikes' (abrupt increases followed by abrupt decreases in the between-map variances of those proportions) (Riitters et al. 2007).

While we do not expect to observe phase transitions occurring at well-defined thresholds on maps with contagion, it is possible that the MSPA pattern classes are more sensitive than other pattern metrics to any phase transitions that do occur. In that case, our approach could be considered along with regression approaches (e.g., Filho and Metzger 2006) as an alternative to the conventional approach to estimating threshold values on maps with contagion. In any case, like With (2002) we can define 'index values' for comparisons, and like Neel et al. (2004) we can make inferences about the effects of contagion on MSPA pattern classes by examining the trends of order parameters in relation to P and H. Knowledge of such effects on neutral maps is needed in order to advance the use of MSPA in application to real landscape problems.

Methods

Generation of neutral maps

Let 'foreground' refer to a focal class of interest, let P be the proportion of a map occupied by foreground, and let H be the measure of contagion of foreground. We used the RULE software (Gardner 1999) to generate neutral foreground maps of size 1,024 × 1,024 pixels. For simple random neutral maps, the presence of foreground was assigned to each pixel independently with probability equal to P. Fifty replicates were considered for each target value of P from 0.01 to 0.99 in steps of size 0.01, providing 4,950 simple random maps for analysis.

Maps with contagion were generated by using the 'multifractal' option in RULE for different combinations of P and H. To generate a 'multifractal' map, RULE first creates a three-dimensional, continuous, fractional Brownian surface by the mid-point displacement algorithm (Fournier et al. 1982; see also Saupe 1988) for a specified H ($0 \leq H \leq 1$), standard deviation of the displacements (in RULE, the standard deviation is always equal to 1.0), and random seed value. The surface is then segmented into foreground and background by selecting a surface 'elevation' in the third dimension for which the proportion of pixels above that elevation is approximately equal to P. The pixels above that elevation are called 'foreground' and those below it are called 'background.' For a given P, a larger value of H produces a map with more clumping of the foreground (Fig. 1). While such maps are directly comparable to earlier studies in landscape ecology that used the RULE software, the algorithm generates non-stationary surfaces that only approximate fractional Brownian surfaces (Mandelbrot 1983, p. 263), which prevents comparisons with exact fractal surfaces (Keitt 2000).

Following preliminary analyses (see below), a set of 11,880 neutral maps with contagion was generated by using the RULE software, consisting of 30 replicates for each combination of P (0.01–0.99 in steps of size 0.01) and H (0.00, 0.10, 0.20, and 0.40). The values of H were in logarithmic progression and did not span the full range of H because there was not much differentiation among MSPA pattern classes for large H (Fig. 1). The actual P on neutral maps differed by a small amount from the target P, and we used the target P when summarizing results later. A
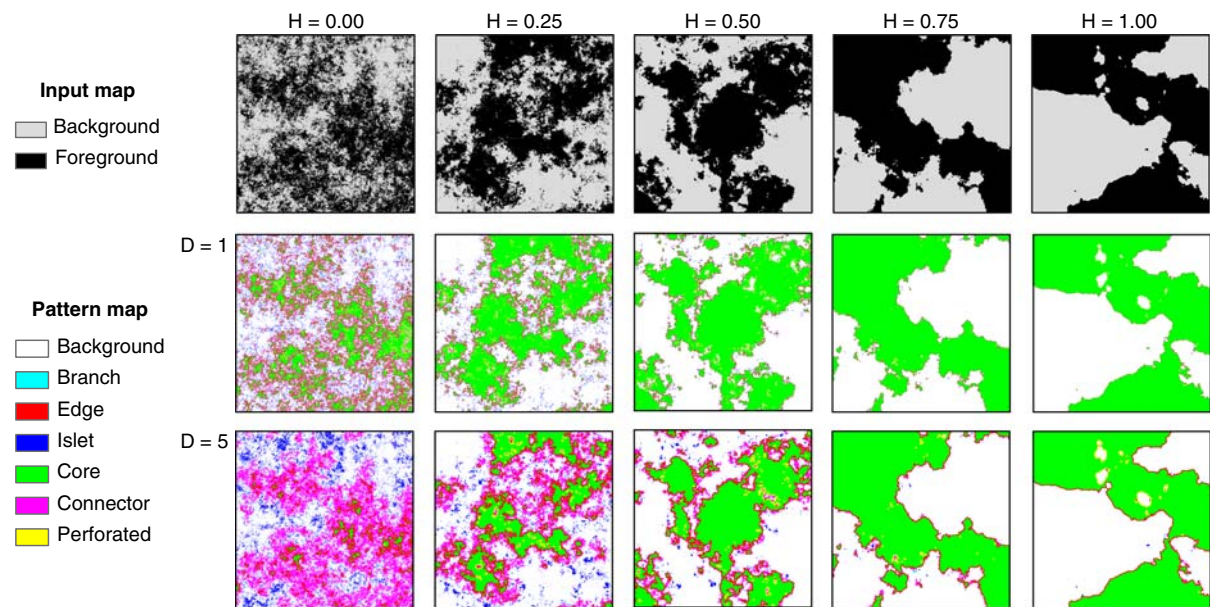
Fig. 1 The *top* row shows examples of maps with 50% foreground (*black pixels*; $P = 0.5$) for five values of the RULE contagion parameter H (contagion increases from *left* to *right*). The *middle* and *bottom* rows illustrate the MSPA pattern classes for those example maps for two edge widths ($D = 1, 5$)

surrounding buffer of background pixels was added to each map before performing the pattern analyses and was subtracted before analyzing the results. Analyses of maps with $P = 0$ and $P = 1$ had trivial results and were not included.

Pattern analysis

The foreground pixels on each map were assigned to one of six mutually exclusive pattern classes (Fig. 1) by using the MSPA algorithm (Soille and Vogt 2009; Vogt 2009). Let D define the edge width, measured in integer multiples of the unit pixel. 'Core' pixels are more than the distance D from background pixels, and are surrounded by 'edge' pixels which form 4-neighbor connected exterior perimeters of width D. Similarly, 'perforated' pixels form 4-neighbor connected interior perimeters of width D that surround holes (background inclusions) in clusters of core. Considering the clusters of foreground that do not contain core, 'connector' pixels form 8-neighbor connected clusters that are 8-neighbor connected to core (through edge or perforated pixels) in at least two places, 'branch' pixels are like connector pixels except the cluster is connected in only one place, and 'islet' pixels are the remaining disjoint clusters of foreground that are too small to contain core pixels.

Following preliminary analyses (see below), the MSPA pattern classes were labeled on each simple random map for four edge widths ($D = 1, 2, 4$, and 5) and on each map with contagion for two edge widths ($D = 1$ and 5). Note that an increase of the edge width is directly related to a decrease of the remaining core area. As will be discussed later, that is important because pattern classes are defined relative to the core pattern class, so the value of D can affect the observation of phase transitions among pattern classes on neutral maps.

Pattern comparisons

For each map, we calculated the proportions of all foreground pixels in each of the six types of pattern classes, and those proportions were the order parameters that were examined for evidence of phase transitions. The sum of all six proportions equaled one for each map, which permitted comparisons of maps with different values of P, H, or D. For the simple random maps, the mean and standard

deviation ($n = 50$ maps) of the proportions were calculated for each target P, for a given D. For the maps with contagion, the mean and standard deviation ($n = 30$ maps) of the proportions were calculated for each combination of H, D, and target P. The trends of those means and standard deviations in relation to P were then examined for evidence of phase transitions. The criteria for declaring a phase transition was the observation of an abrupt change in one or more of the mean values, accompanied by the observation of between-map variance spikes.

Preliminary and supplementary analyses

Several preliminary and supplementary analyses are summarized briefly here. It was mentioned that the MSPA algorithm (Soille and Vogt 2009) differed from the algorithm (Vogt et al. 2007a, b) that was used for the earlier neutral model analysis of simple random maps (Riitters et al. 2007). As a preliminary analysis to identify the impacts of those changes on previous results, we repeated the earlier analysis of simple random maps. Apart from the differences between 4-neighbor connectivity (previous study) and 8-neighbor connectivity (present study) that are expected from percolation theory, changes to the MSPA definitions of the 'structuring element' and the perforated pattern class shifted the phase transition between the edge and perforated pattern classes to larger threshold P values.

A supplementary analysis of maps with contagion considered two more edge widths ($D = 2$ and 4) and two more levels of contagion ($H = 0.05$ and 0.80). Those results were omitted to save space. In addition, because Mandelbrot (1983, p. 266) suggested that phase transitions may occur at threshold values of H (not P), we evaluated a set of maps with contagion comprising 30 replicates for each combination of H (0.00 to 1.00 in steps of size 0.01) and P (0.10, 0.20, 0.40, 0.50, 0.60, and 0.80). The results of that analysis did not substantiate phase transitions at threshold H values.

Finally, for RULE-generated maps with contagion, maps with the same values of P and H differ because the value of the random seed defines a unique three-dimensional surface (see above). Because such surfaces are not stationary (Keitt 2000), raising or lowering the 'elevation' on the same surface (i.e., by using the same seed value) could precipitate phase

transitions that are masked by varying the elevation on an 'average surface' (i.e., by using different seed values). Since we used a different seed value for each map, we evaluated that possibility by generating maps using the same seed value while varying P for a given H, essentially changing the 'elevation' on the same surface as P was varied from 0.01 to 0.99 in steps of size 0.01. We repeated that procedure for 30 seed values for $H = 0.00$, 0.10, 0.20, and 0.40 and visually inspected the resulting trends of the MSPA pattern classes in relation to P for each surface. The trends for each surface were similar to the average trends as reported in this study.

Results and discussion

Phase transitions on simple random maps

On simple random maps, the occurrence and relative abundance of different pattern classes were strongly related to P and D, and phase transitions were signaled by abrupt shifts in the proportions of pixels in different pattern classes and by variance spikes (Fig. 2). The phase transition between the islet pattern class and the connector plus branch pattern classes was interpreted by using the same logic as Riitters et al. (2007) as follows. By definition in MSPA, connector and branch pixels do not exist unless core pixels exist, and therefore the existence of core pixels is a prerequisite to phase transitions involving the connector and branch pattern classes. On the sample maps, the first core pixels emerged at $P \approx 0.20$, 0.55, 0.78 and 0.87 for $D = 1$, 2, 4, and 5, respectively. A larger P was needed for a larger D because the existence of core required larger clusters when the edge width was wider. In comparison, percolation theory guaranteed the formation of a map-spanning cluster of 8-neighbor connected foreground at $P \approx 0.41$ (e.g., Plotnick and Gardner 1993). Therefore, for $D = 2$, 4, and 5, the phase transition from the islet pattern class to the connector plus branch pattern classes was precipitated by the first emergence of the core pattern class on maps that already contained a map-spanning cluster, and threshold P values corresponded to the emergence of the core pattern class. For $D = 1$, the same phase transition was precipitated by the emergence of the map-spanning cluster on maps that already contained

the core pattern class, at a threshold $P \approx 0.41$ as predicted by percolation theory.

The phase transition between the edge and perforated pattern classes was also interpreted by using the same logic as before. Let P_c be the proportion of the map (foreground plus background) that comprises the core pattern class. With increasing P, the phase transition occurred at the value of P for which P_c first exceeded 0.41, which corresponded to the formation of a (4-neighbor connected) map-spanning cluster of non-core foreground plus non-foreground pixels. At the phase transition, the local context of the background pixels changed abruptly from exterior to interior. The foreground pixels that were formerly in the edge pattern class (i.e., perimeter of core adjacent to exterior background) became the perforated pattern class (i.e., perimeter of core adjacent to interior background). Variance spikes were evident (Fig. 2) only for $D = 1$ and 2. For $D = 4$, the phase transition occurred at $P = 0.99$ and the variance spike was not visually evident. There was no phase transition for $D = 5$ because P_c did not exceed 0.41 when $P = 0.99$.

In summary, two types of phase transitions among MSPA pattern classes occurred on simple random neutral maps at threshold P values expected from percolation theory in light of the connectivity rule and edge width employed in the MSPA algorithm. For later comparisons to maps with contagion, note that a phase transition implies the intersection of two trend lines (Fig. 2) at some threshold P value. Also note that with increasing P, the progressions of map dominance by different pattern classes were similar for all D. As P increased from zero, maps that were dominated by small and disconnected clusters of foreground (islet pattern class) became dominated by the pattern classes that form paths between clusters of the core pattern class (connector and branch pattern classes) at intermediate values of P, and ultimately by the pattern classes associated with large clusters of foreground (core, edge, and perforated pattern classes) at high values of P.
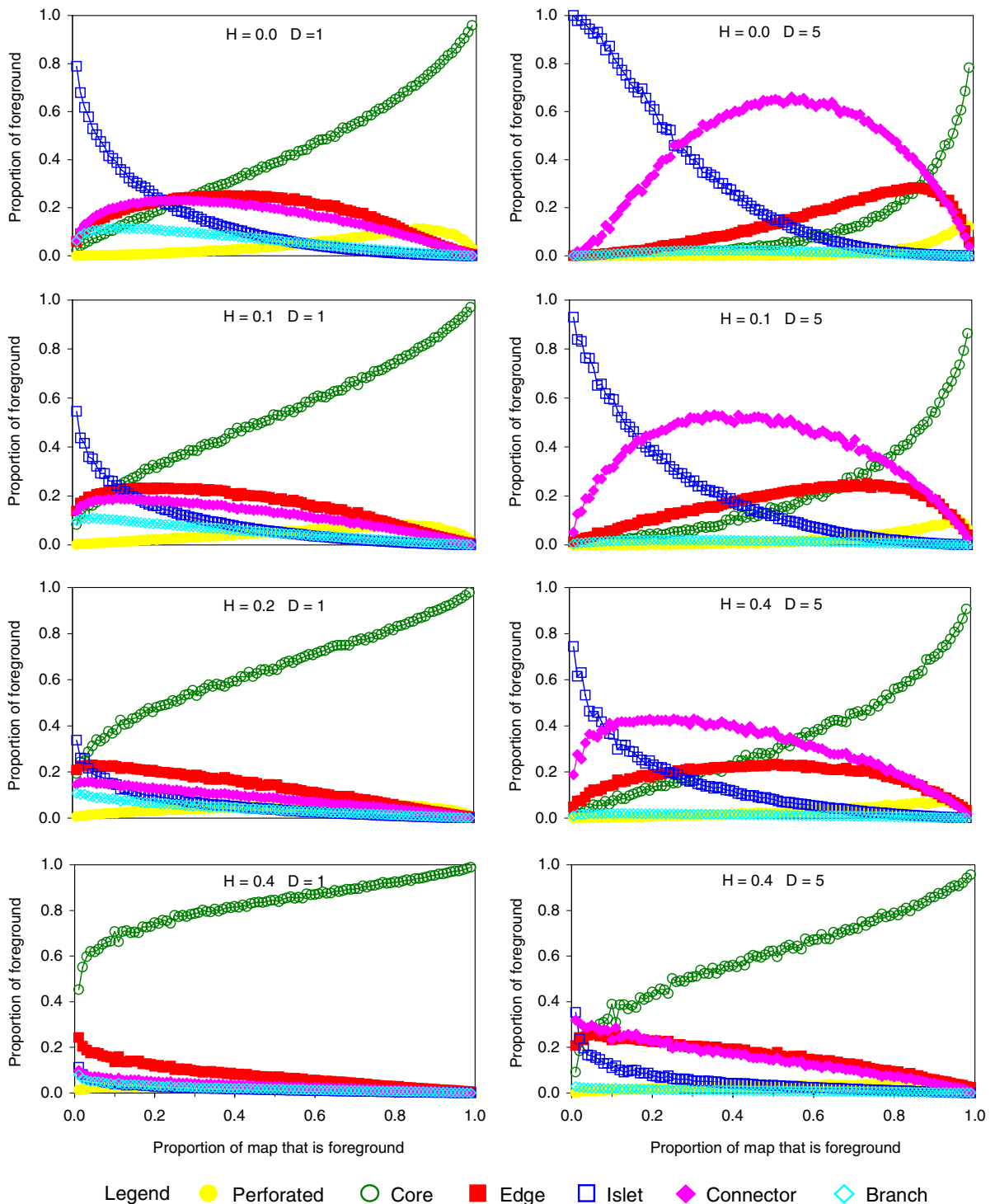
Neutral maps with contagion

The occurrence and relative abundance of MSPA pattern classes on maps with contagion were related to P, H, and D (Fig. 3). For relatively large contagion ($H = 0.40$), the maps tended to be dominated over
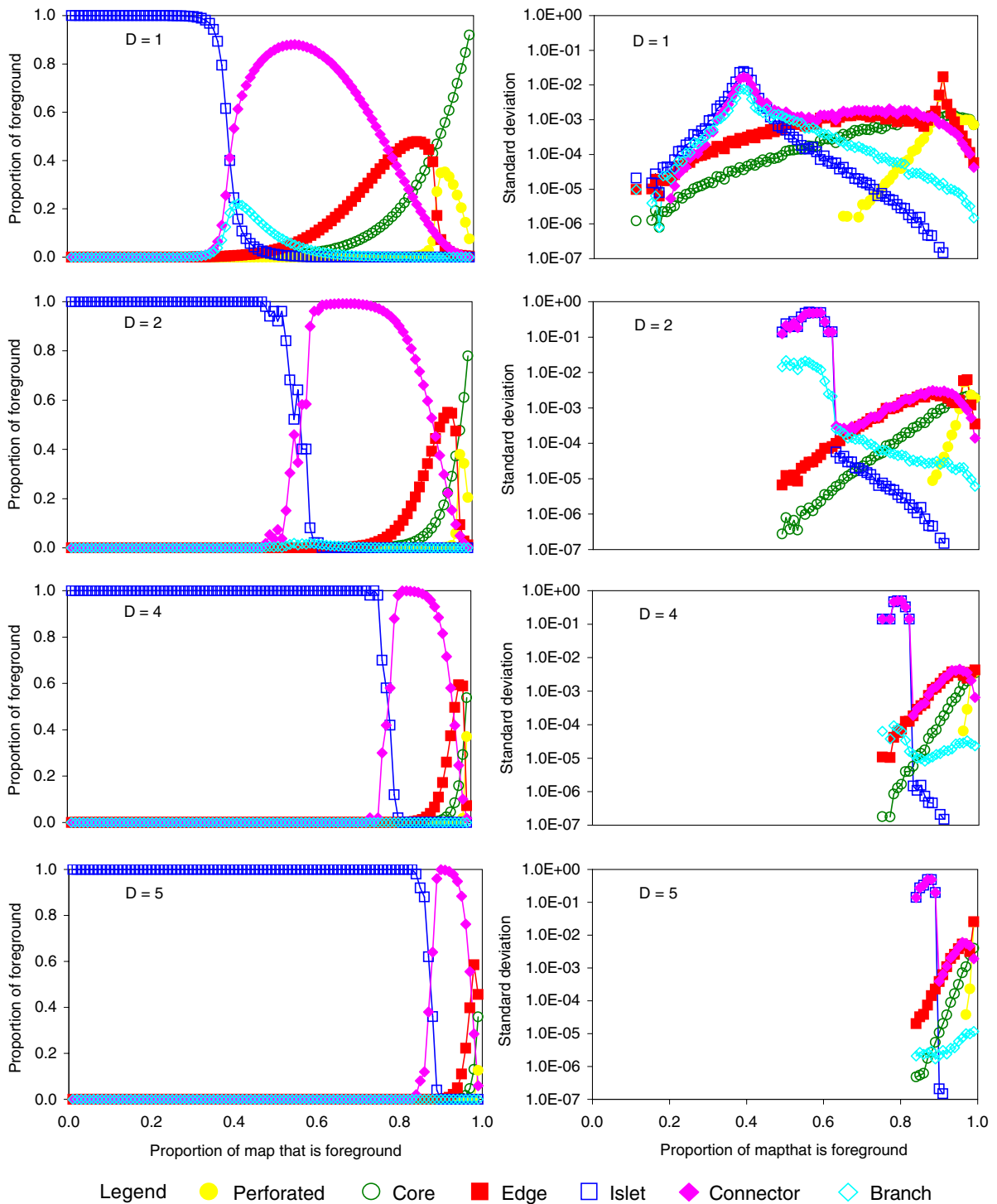
Fig. 2 Summary of MSPA pattern classes on simple random neutral maps. *Left*: the mean proportions of the foreground in each of the six pattern classes. *Right*: the standard deviations of those proportions. The *horizontal axes* are the proportion (*P*) of the map that is foreground. From *top* to *bottom*, the edge width (*D*) indicates the four scales of analysis. The mean and standard deviation for a given value of *P* are based on 50 maps

Fig. 3 Summary of MSPA pattern classes on neutral maps with contagion. The mean proportions of the foreground in each of the six pattern classes are shown for four values of contagion (*H*; *top* to *bottom*) and two edge widths (*D*; *left* to *right*), in relation to the proportion of the map that is foreground (*P*; *all horizontal axes*). Each data point is the mean of 30 maps

the full range of P by the core, edge, and connector pattern classes, consistent with earlier observations that such maps contain a few large, tightly packed, and connected clusters of foreground (e.g., Ferrari et al. 2007). With increasing D for large H, the core pattern class was replaced by the edge and connector pattern classes because an increase in the edge width necessarily resulted in a larger edge-to-core ratio, and because the wider edges subdivided some of the core clusters into pieces that were still connected to each other.

Maps with smaller contagion ($H \leq 0.10$) exhibited more differentiation of pixels among pattern classes over wider ranges of P (Fig. 3). When H and P were both small, the maps were dominated by the islet class which indicated that the clusters of foreground were relatively small and disjoint. With increasing P, the connector class became more abundant at the expense of the islet class. The connector-to-core ratio was relatively large, indicating that only a small number of the islet clusters of foreground became large enough to be core, and when that occurred, there was usually a pathway between those clusters. Additional increases in P resulted in the formation of more of the core class and its associated edge class, which tended to replace the islet class instead of the connector class. For the largest values of P, the foreground typically formed a single large cluster that occupied most of the map, and as a result, the maps became dominated by the core class which replaced both the connector and edge classes. Increasing D for small H affected primarily the pixels that were in the core class when $D = 1$, which became connector and edge pixels when $D = 5$, for the same reasons as mentioned earlier. The perforated and branch classes were minor components of pattern in all but a few cases, which indicated that maps with contagion did not typically exhibit holes in clusters of foreground, or incomplete paths between clusters of core.

Unlike simple random maps, there was no compelling evidence of phase transitions on maps with contagion. The transitions among the pattern classes on maps with contagion were gradual (Fig. 3), not abrupt (Fig. 2), and there were no variance spikes (results not shown). At the same time, the shifts in map dominance by different pattern classes with increasing P were similar to the characteristics of simple random maps. That suggested the possibility of using index values for the purpose of comparing

the effects of contagion and edge width. For example, With and King (1997) reported that 'threshold values' of P (i.e., their index values) decreased with H, occurring at $P = 0.50$ for $H = 0.01$ and at $P = 0.44$ for $H = 0.99$ for the maps that they tested. In contrast, Ferrari et al. (2007) examined similar maps with a different order parameter and reported that 'threshold values' increased with H, from $P = 0.15$ to 0.30 for $H = 0.00$, to $P = 0.50$ to 0.70 for $H = 1.00$.

We defined index P values for comparing the effects of contagion and edge width as follows. Recall that for simple random maps, the phase transitions were either precipitated by the formation of a map-spanning cluster, or they were translated to a larger threshold P at which the core class first emerged within a map-spanning cluster. For the maps with contagion, the core class was always present at all values of P (Fig. 3), and as a result, threshold P values (if any) depended only on H and D. Noting that a phase transition implied the intersection of two trend lines (Fig. 2), and that there were two phase transitions, we defined one index as the value of P at which the proportion of the islet class equaled the proportion of the connector class, and another index as the value of P at which the proportion of the edge class equaled the proportion of the perforated class.

In comparison to simple random maps (Fig. 2), those index values occurred at lower values of P on maps with contagion (Fig. 3). Furthermore, with H increasing from 0.00 to 0.10, the intersections occurred at even smaller values of P for a given D, and if H became large enough for a given D, then the intersections were not obtained (Fig. 3). Our observation that index values decreased with increasing H was consistent with the findings of With and King (1997). Furthermore, if contagion "dampened" phase transitions (Neel et al. 2004), and even the smallest value of contagion ($H = 0.00$) reduced threshold P values (compare Figs. 2 and 3), then it was logical that larger values of contagion should result in more "dampening" and thus, lower index P values as we observed.

In contrast, the index values increased with D for a fixed H (Fig. 3), which means that the effect of a wider edge width was opposite the effect of higher contagion. That explains why the results for the simple random maps appeared to be most similar to the results for the maps with the least contagion

($H = 0.00$) and widest edges ($D = 5$). Thus, it may be anticipated that phase transitions could be obtained on maps with contagion if the edge width is 'large enough,' reasoning that no matter how the foreground pixels are distributed, the distribution of the core pattern class can appear to be random (and thus, potentially involved in a phase transition) if the individual clusters of the core are 'small enough.' That could have ecological implications if, for example, organism movement through 'core habitat' is functionally different from movement through 'edge habitat' (Malanson 2003).

Conclusion

Gardner and Urban (2007) stated that inferences about landscape pattern and process will not be very satisfying at high values of P, in part because "percolation theory defines a boundary above which few differences exist between random and real landscapes." They suggested that studies of landscape patterns would be more productive at lower values of P and that if the foreground P was large, then the patterns of the background should be examined instead. In contrast, our investigations of landscape patterns from MSPA showed clear and large differences between foreground patterns on maps with large P. Furthermore, we have shown that percolation theory defines several 'boundaries' and that one of them is located at high values of P. Inferences about landscape pattern and process are potentially satisfying only if the landscape pattern metrics are sensitive to changes in pattern and phase transitions in the range of P that is of interest, which is not the case for many classical pattern metrics when P is large (Neel et al. 2004). Pattern metrics from MSPA should prove useful for investigating ecological processes even when P is large, if those processes depend on connectedness as influenced by the existence of core, edge, perforated, connector, branch, and islet patterns, which is likely the case for the classical ecological problem addressing organism movement within and between landscapes.

Neutral maps with and without contagion will continue to be useful as test-beds for exploring differential sensitivities and responses of pattern metrics within the metric space defined by P and H (e.g., Neel et al. 2004), but samples of real maps are

sometimes advocated to extend results to more aspects of pattern (e.g., Cushman et al. 2007). In the real world, phase transitions are contingent on initial conditions and are driven by the pattern of changes from foreground to background (Filho and Metzger 2006). If the MSPA pattern metrics were applied (with an appropriate edge width) to a temporal series of real maps, we expect that landscapes experiencing a random pattern of change will exhibit phase transitions among the MSPA pattern classes, irrespective of initial conditions. The threshold values will be as described in the present study, except they will apply to the proportion of the original foreground, instead of the proportion of the entire map. On the other hand, we do not expect to observe phase transitions of MSPA pattern classes on any map, irrespective of initial conditions, if the patterns of change are clumped, contagious, linear, or otherwise not random.

References

Burkett VR, Wilcox DA, Stottlemyer R, Barrow W, Fagre D, Baron J, Price J, Nielsen JL, Allen CD, Peterson DL, Ruggerone G, Doyle T (2005) Nonlinear dynamics in ecosystem response to climatic change: case studies and policy implications. Ecol Complex 2:357–394. doi: 10.1016/j.ecocom.2005.04.010

Chaves CM, Koiller B (1995) Universality, thresholds and critical exponents in correlated percolation. Physica A 218:271–278. doi:10.1016/0378-4371(95)00076-J

Cushman SA, McGarigal K, Neel MC (2007) Parsimony in landscape metrics: strength, universality, and consistency. Ecol Indic 8:691–703. doi:10.1016/j.ecolind.2007.12.002

Essam JW (1980) Percolation theory. Rep Prog Phys 43:833–912. doi:10.1088/0034-4885/43/7/001

Ferrari JR, Lookingbill TR, Neel MC (2007) Two measures of landscape-graph connectivity: assessment across gradients in area and configuration. Landscape Ecol 22:1315–1323. doi:10.1007/s10980-007-9121-7

Filho FJBdO, Metzger JP (2006) Thresholds in landscape structure for three common deforestation patterns in the Brazilian Amazon. Landscape Ecol 21:1061–1073. doi: 10.1007/s10980-006-6913-0

Fournier A, Fussel D, Carpenter L (1982) Computer rendering of stochastic models. Commun ACM 25:371–384. doi: 10.1145/358523.358553

Frary ME, Schuh CA (2007) Correlation-space description of the percolation transition in composite microstructures. Phys Rev E Stat Nonlin Soft Matter Phys 76:041108. doi:10.1103/PhysRevE.76.041108

Gardner RH (1999) RULE: a program for the generation of random maps and the analysis of spatial patterns. In: Klopatek JM, Gardner RH (eds) Landscape ecological analysis: issues and applications. Springer-Verlag, New York, pp 280–303

Gardner RH, Urban DL (2007) Neutral models for testing landscape hypotheses. Landscape Ecol 22:15–29. doi:10.1007/s10980-006-9011-4

Gardner RH, Milne BT, Turner MG, O'Neill RV (1987) Neutral models for the analysis of broad-scale landscape pattern. Landscape Ecol 1:19–28. doi:10.1007/BF02275262

Gardner RH, O'Neill RV, Turner MG, Dale VH (1989) Quantifying scale-dependent effects of animal movement with simple percolation models. Landscape Ecol 3:217–227. doi:10.1007/BF00131540

Groffman PM, Baron JS, Blett T, Gold AJ, Goodman I, Gunderson LH, Levinson BM, Palmer MA, Paerl HW, Peterson GD, Poff NL, Rejeski DW, Reynolds JF, Turner MG, Weathers KC, Wiens J (2006) Ecological thresholds: the key to successful environmental management or an important concept with no practical application? Ecosystems (N Y, Print) 9:1–13. doi:10.1007/s10021-003-0142-z

Gustafson EJ, Parker GR (1992) Relationships between land-cover proportion and indices of landscape spatial pattern. Landscape Ecol 7:101–110. doi:10.1007/BF02418941

Keitt TH (2000) Spectral representation of neutral landscapes. Landscape Ecol 15:479–493. doi:10.1023/A:1008193015770

King AW, With KA (2002) Dispersal success on spatially structured landscapes: when do spatial pattern and dispersal behavior really matter? Ecol Model 147:23–39. doi:10.1016/S0304-3800(01)00400-8

Malanson GP (2003) Dispersal across continuous and binary representations of landscapes. Ecol Model 169:17–24. doi:10.1016/S0304-3800(03)00204-7

Mandelbrot BB (1983) The fractal geometry of nature. W.H Freeman and Company, New York, p 468

Neel MC, McGarigal K, Cushman SA (2004) Behavior of class-level landscape metrics across gradients of class aggregation and area. Landscape Ecol 19:435–455. doi:10.1023/B:LAND.0000030521.19856.cb

O'Neill RV, Milne BT, Turner MG, Gardner RH (1988) Resource utilization scales and landscape pattern. Landscape Ecol 2:39–63. doi:10.1007/BF00138908

O'Neill RV, Gardner RH, Turner MG (1992) A hierarchical neutral model for landscape analysis. Landscape Ecol 7:55–61. doi:10.1007/BF02573957

Ostapowicz K, Vogt P, Riitters KH, Kozak J, Estreguil C (2008) Impact of scale on morphological spatial pattern of forest. Landscape Ecol 23:1107–1117. doi:10.1007/s10980-008-9271-2

Plotnick RE, Gardner RH (1993) Lattices and landscapes. In: Gardner RH (ed) Lectures on mathematics in the life sciences, Volume 23: predicting spatial effects in ecological systems. American Mathematical Society, Providence, RI, pp 129–157

Riitters KH, Vogt P, Soille P, Kozak J, Estreguil C (2007) Neutral model analysis of landscape patterns from mathematical morphology. Landscape Ecol 22:1033–1043. doi:10.1007/s10980-007-9089-3

Saupe D (1988) Algorithms for random fractals. In: Peitgen HO, Saupe D (eds) The science of fractal images. Springer-Verlag, New York, pp 71–136

Serra J (1982) Image analysis and mathematical morphology. Academic Press, London

Soille P (2003) Morphological image analysis: principles and applications, 2nd edn. Springer-Verlag, Berlin

Soille P, Vogt P (2009) Morphological segmentation of binary patterns. Pat Recog Let 30:456–459. doi:10.1016/j.patrec.2008.10.015

Stauffer D (1985) Introduction to percolation theory. Taylor & Francis, London

Vogt P (2009) GUIDOS installation. European Commission, Joint Research Centre, Ispra, Italy, 4 pp. (online) URL: http://forest.jrc.ec.europa.eu/biodiversity/GUIDOS/ (accessed 29 January 2009)

Vogt P, Riitters KH, Estreguil C, Kozak J, Wade TG, Wickham JD (2007a) Mapping spatial patterns with morphological image processing. Landscape Ecol 22:171–177. doi:10.1007/s10980-006-9013-2

Vogt P, Riitters KH, Iwanowski M, Estreguil C, Kozak J, Soille P (2007b) Mapping landscape corridors. Ecol Indic 7:481–488. doi:10.1016/j.ecolind.2006.11.001

With KA (2002) Using percolation theory to assess landscape connectivity and effects of habitat fragmentation. In: Gutzwiller KJ (ed) Applying landscape ecology in biological conservation. Springer-Verlag, New York, pp 105–130

With KA (2004) Assessing the risk of invasive spread in fragmented landscapes. Risk Anal 24:803–815. doi:10.1111/j.0272-4332.2004.00480.x

With KA, King AW (1997) The use and misuse of neutral landscape models in ecology. Oikos 79:219–229. doi:10.2307/3546007

With KA, King AW (2001) Analysis of landscape sources and sinks: the effect of spatial pattern on avian demography. Biol Conserv 100:75–88. doi:10.1016/S0006-3207(00)00209-3